



AFIT/GAE/AA/78D-2



TWO-DIMENSIONAL SUPERSONIC  
JET MIXING OF AIR AND HELIUM

THESIS

AFIT/GAE/AA/78D-2 ✓

Roy L. Bonney  
Captain USAF

Approved for public release; distribution unlimited.

14)

AFIT/GAE/AA/78D-2

6)

TWO-DIMENSIONAL SUPERSONIC  
JET MIXING OF AIR AND HELIUM

9) Master's THESIS

Presented to the Faculty of the School of Engineering  
of the Air Force Institute of Technology  
Air Training Command  
in Partial Fulfillment of the  
Requirements for the Degree of  
Master of Science

12) 5'

by

10)

Roy L. Bonney, B.S.  
Captain USAF

Graduate Aeronautical Engineering

11)

Dec ~~1978~~ 78

Accession	
NTIS	
DDC	
Unannounced	
Special	
Other	
A	

Approved for public release; distribution unlimited.

012225

## Preface

This study is a result of the continued interest in the development of high energy gasdynamic lasers. It is a continuation of a study initiated by Dr. A. J. Shine of the Air Force Institute of Technology. The basic equipment that was used during my experiments, was designed and built by Captain John D. Carlile, AFIT class GAE-78M.

This thesis presents the results of my experimental efforts in analyzing the mixing and flow characteristics of helium and air downstream of a two-dimensional array of supersonic nozzles. The data was taken in the form of schlieren photographs, pressure measurements, and gas samples. The study was limited to an investigation of turbulent mixing at various nozzle exit pressure ratios.

I wish to thank Dr. Richard A. Merz for his valuable guidance and able assistance throughout my study. I also appreciate the help of Drs. William C. Elrod, Harold E. Wright, and Robert L. Roach. A special thanks is given to the skilled craftsmen of the AFIT Model Shop for their outstanding service and excellent workmanship. The assistance of Mr. William Baker and Mr. Harold Cannon most certainly will be remembered. Last, but most important, I wish to thank my wife, Carol, for her help and understanding during this academic endeavor.

Roy L. Bonney

Contents

	<u>Page</u>
Preface . . . . .	ii
List of Figures . . . . .	v
List of Symbols . . . . .	vii
Abstract . . . . .	ix
I. Introduction . . . . .	1
Background . . . . .	1
Purpose and Scope . . . . .	3
Assumptions . . . . .	4
II. Experimental Equipment . . . . .	5
Test Section . . . . .	5
Air Supply . . . . .	6
Air Stilling Chamber . . . . .	6
Helium Supply . . . . .	7
Helium Stilling Chamber . . . . .	7
Schlieren System . . . . .	7
Vacuum System . . . . .	8
Gas Sample Collection System . . . . .	8
Pressure Measurements . . . . .	9
Instrumentation . . . . .	9
III. Experimental Procedure . . . . .	11
IV. Discussion of Results . . . . .	14
Test Conditions . . . . .	14
Pressure Measurement Analysis . . . . .	15
Schlieren Analysis . . . . .	15
Gas Sampling Analysis . . . . .	17
V. Conclusions . . . . .	20
VI. Recommendations . . . . .	21
Figures . . . . .	22
References . . . . .	41

Contents

	<u>Page</u>
Appendix A: Gas Sample Pressure Calculation . . . . .	42
Appendix B: Calculation of Masses and Mole Fractions .	45
Vita . . . . .	46

List of Figures

<u>Figure</u>		<u>Page</u>
1	Flow Field Schematic . . . . .	22
2	Test Equipment Schematic . . . . .	23
3	Test Section Schematic Showing Probe Positions . . . . .	24
4	Photograph of Test Section . . . . .	25
5	Photograph of Test Apparatus . . . . .	25
6	Gas Sampling and Pressure Measurement Configuration . . . . .	26
7	Variation of $P_t/P$ Across the Flow Field for Several Downstream Locations, $Pr = 1.95$ . . . . .	27
8	Variation of $P_t/P$ Across the Flow Field for Several Downstream Locations, $Pr = 2.50$ . . . . .	28
9	Variation of $P_t/P$ Across the Flow Field for Several Exit Plane Pressure Ratios, $x/D = 1.29$ (Position A) . . . . .	29
10	Variation of $P_t/P$ Across the Flow Field for Several Exit Plane Pressure Ratios, $x/D = 4.74$ (Position C) . . . . .	30
11	Mixing Geometry and Jet Core Schematic . . . . .	31
12	Schlieren Photograph of Flow Field, $Pr = 2.0$ , Knife Edge Perpendicular to Flow . . . . .	32
13	Schlieren Photograph of Flow Field, $Pr = 2.5$ , Knife Edge Perpendicular to Flow . . . . .	32
14	Schlieren Photograph of Flow Field, $Pr = 1.3$ , Knife Edge Parallel to Flow . . . . .	33
15	Schlieren Photograph of Flow Field, $Pr = 2.8$ , Knife Edge Parallel to Flow . . . . .	33
16	Mole Fraction Variation of Air and Helium Across Flow Field for Several Values of Exit Plane Pressure Ratios, $x/D = 6.47$ (Position D) . . . . .	34

<u>Figure</u>	<u>Page</u>
17	Mole Fraction Variation of Air and Helium with Exit Plane Pressure Ratios, $x/D = 1.29$ (Position A) . . . . . 35
18	Mole Fraction Variation of Air and Helium with Exit Plane Pressure Ratios, $x/D = 3.02$ (Position B) . . . . . 36
19	Mole Fraction Variation of Air and Helium with Exit Plane Pressure Ratios, $x/D = 4.74$ (Position C) . . . . . 37
20	Mole Fraction Variation of Air and Helium with Exit Plane Pressure Ratios, $x/D = 6.47$ (Position D) . . . . . 38
21	Mole Fraction Variation of Air and Helium with Exit Plane Pressure Ratios, $x/D = 8.19$ (Position E) . . . . . 39
22	Mole Fraction Variation of Air and Helium with Exit Plane Pressure Ratios, $x/D = 9.91$ (Position F) . . . . . 40
A1	Schematic of Gas Sample Bottle Pressure Measurement Configuration . . . . . 44

## List of Symbols

<u>Symbol</u>	<u>Definition</u>
A	Volume per length of manometer
b	Distance from nozzle exit to maximum core width position
D	Air nozzle width at exit plane
h	Gage pressure
$h_o$	Distance from bottle to zero position of manometer
$M_A$	Fraction of air by mass
$M_H$	Fraction of helium by mass
$m_A$	Mass of 100% air at the pressure and temperature under investigation
$m_H$	Mass of 100% helium at the pressure and temperature under investigation
$N_A$	Mole fraction of air
$N_H$	Mole fraction of helium
P	Local static pressure
$P_A$	Static air pressure at nozzle exit
$P_H$	Static helium pressure at nozzle exit
$P_t$	Local total pressure
$P_1$	Pressure in sample bottle and manometer
$P_2$	Pressure in sample bottle only
Pr	Ratio of $P_A$ to $P_H$
$V_1$	Volume of sample bottle and manometer
$V_2$	Volume of sample bottle only

Symbol

Definition

w	Maximum jet core width
x	Coordinate parallel to flow direction
$x_m$	Mixing length of air jet
y	Coordinate perpendicular to flow direction
$\theta$	Spreading angle of mixing face

### Abstract

This study investigated the mixing and flow field characteristics of helium and air using an array of two-dimensional Mach 3.0 nozzles. The study made use of schlieren photography, pressure measurements, and gas sampling for the analysis. Exit plane pressure ratios from 1.0 to 3.0 were investigated. Exit velocity ratios were assumed constant for all test conditions. Test equipment consisted of the nozzle array installed in a blow-down type system. Static pressure taps and total pressure probes were installed in the flow field downstream of the mixing nozzles to measure pressures. The probes were also used to capture gas samples. Pressure measurement results showed symmetry of the flow field. Gas samples and schlieren analysis indicated that mixing was a function of exit plane pressure ratio and distance from nozzle exit.

TWO-DIMENSIONAL SUPERSONIC  
JET MIXING OF AIR AND HELIUM

I. Introduction

Background

In a continuing search for improved and more sophisticated weapon systems, the Air Force Weapons Laboratory at Kirtland AFB, New Mexico, requested support from the Air Force Institute of Technology on an investigation of the gasdynamic laser.

Gasdynamic laser operation is based on the rapid expansion of a high temperature and high pressure gas through a supersonic nozzle (or nozzles) to relatively high Mach numbers. This lowers the gas temperature and pressure downstream of the nozzle (Ref 1). The translational and rotational energy of the gas is rapidly lost through molecular collisions when the temperature is suddenly reduced. However, the vibrational energy is not so easily dissipated and the number of molecules in the upper energy states exceed the number of molecules in the lower energy states producing what is termed a population inversion (Ref 2). (Normally the number of molecules in the lower energy states exceed the number in the higher energy states).

The addition of water vapor or helium to the gas increases the population inversion by causing some of the

lower energy states to decay more rapidly (Ref 3). It has been found that by mixing the water vapor or helium during or after expansion of the gas, longer vibrational relaxation times are produced and higher energy lasing is possible.

Although mixing after expansion produces more available energy, extracting this energy from a laser cavity is limited by several factors. Turbulence and shock waves created by the nozzles and their wakes can affect the optical quality of the laser beam and create losses due to beam divergence. These losses can be reduced by decreasing the turbulent density fluctuations of the flow field. Gas mixture concentrations also affects total power output. A loss of energy can be expected if the gases are only partially mixed. The mixing must also be completed in a time shorter than the vibrational relaxation time of the upper energy states. Therefore, it is important to have complete mixing in a relatively short time to minimize energy losses in the laser cavity.

Borghini, et al., (Ref 4) and Cassidy, et al., (Ref 5) investigated different nozzle designs in their attempt to improve the gain of the laser cavity. They, as well as others, were primarily interested in the overall gain of the laser and not in the fluid dynamics of the flow field. Peterson (Ref 6) concentrated his efforts on measurement of flow field properties but did not analyze the mixing of dissimilar gases.

Other studies on mixing were mostly theoretical in nature with very little applicable experimental work accomplished (Ref 7, 8, 9). The experimental work that was accomplished generally related to other fields such as propulsions and ignored problems that are characteristic of laser cavities.

This study investigates the mixing of two dissimilar gases (helium and air) as it relates to gasdynamic lasers. Complications caused by chemical reactions and high temperatures were absent. The primary consideration was to determine the turbulent mixing characteristics of the two gases for a given mixing nozzle array. This was done by analyzing gas samples to determine the helium and air mole fractions. Equipment limitations prevented any major temperature difference in the two gases. Therefore, the exit velocity ratio was considered approximately constant for all test conditions. The static pressure ratio between nozzle exit planes was chosen as the independent variable.

#### Purpose and Scope

The purpose of this study was to investigate the mixing and flow characteristics of a two-dimensional array of supersonic mixing nozzles which utilize air and helium as the two mixing gases. A schematic of the flow field showing the shear regions and shock patterns is shown in Figure 1. This is a continuation of a study by Carlile (Ref 10), who designed the basic apparatus used in this study.

The scope of this study was to; (1) conduct a brief literature review on the mixing of gases in supersonic flow; (2) evaluate the facility designed by Carlile and make necessary changes in the facility where needed; (3) compare the flow field at various nozzle exit pressure ratios using static and total pressure measurements and schlieren photography; (4) sample and analyze the gas mixture at various locations across the flow field downstream of the nozzles.

#### Assumptions

Air and helium were assumed to obey the perfect gas law in the temperature and pressure ranges of this study. The nozzles are assumed to behave isentropically for simplicity of calculations.

## II. Experimental Equipment

The experimental equipment used in this study consisted of a test section, an air supply, a helium supply, an air stilling chamber, a helium stilling chamber, a schlieren system, a vacuum system, a gas sample collection system, and other instrumentation. A schematic of the equipment is given in Figure 2.

### Test Section

The test section consisted of two helium nozzles sandwiched between three air nozzles as shown in Figure 1. This arrangement was chosen to produce a more realistic boundary condition for the two central mixing regions. In application the mixing arrangement would have a large number of alternating helium and air nozzles.

The helium and air nozzles were both machined from aluminum and designed to produce two-dimensional flow with a nominal exit Mach number of 3.0. The helium nozzle throat measured 0.10 inches with its exit measuring 0.281 inches. The air nozzle throat measured 0.131 inches with the exit measuring 0.567 inches. Both nozzles had a depth of 0.375 inches. Although the depth was enough to provide good two-dimensional flow, it wasn't sufficient to show the density gradients in the helium using the schlieren analysis. (The helium was found to be supersonic downstream of the nozzle using pressure measurements).

The test cavity was 7 inches long, 2.375 inches wide, and .375 inches deep and was made of 0.75 inch clear plexiglass. One sidewall had static pressure taps located in the exit plane of each nozzle on its centerline. The other sidewall was interchangeable. A clear sidewall was used for schlieren photographs while a sidewall containing pressure taps and probe ports was used for gas sampling and pressure measurements. The location of the pressure taps are shown in Figure 3. The test section is shown in Figure 4 while Figure 5 shows the test apparatus.

#### Air Supply

Air was supplied to the system by two 100 HP Worthington air compressors. The air from the compressors was dried and filtered before being stored in the supply tanks. A manually operated slide valve regulated the pressure to a manually operated quick opening gate valve that was connected to the inlet of the air stilling chamber.

#### Air Stilling Chamber

The air from the supply was brought to the stilling chamber through a 4 inch flexible supply line. The stilling chamber was cylindrical with a diameter of 13 inches and a length of 48 inches. The filter at the exit of the stilling chamber removed any small dust particle in the air before entering the test section.

### Helium Supply

Helium was supplied from a bank of twelve high pressure bottles connected to a common manifold. The pressure was regulated by two dome valves and the flow was controlled by a manually operated fast acting ball valve.

The helium was brought to the helium stilling chamber by a 0.5 inch flexible tube.

### Helium Stilling Chamber

The helium chamber was a cylinder 36 inches long and 2.5 inches in diameter. A filter and screen were located at its center section. The helium was fed to the test section through four lengths of 0.375 inch flexible tubing.

### Schlieren System

A schlieren system and camera were used to view and photograph the flow field in the test section. Two 7 inch parabolic mirrors with a 40 inch focal length were used to reflect light through the test section. For real time observations, a zirconium arc lamp provided a continuous light source and the image was projected onto a frosted glass screen for visualization. A Graflex camera with Polaroid, Type 47, film was used with a spark lamp light source for all schlieren photographs. The spark duration was approximately 0.2 milliseconds. Photographs were taken at each flow condition with the knife edge both perpendicular and parallel to the flow direction.

### Vacuum System

One Stokes and two Leiman vacuum pumps were used in parallel to evacuate sixteen 33.4 cubic foot storage tanks. The vacuum system was adequate to maintain a pressure of at least 20 inches of Hg. below atmospheric for the duration of each test condition. The vacuum pumps were also used to evacuate the gas sample bottles to an absolute pressure of less than 0.2 inches of Hg. The vacuum system, when used in conjunction with the pressurized air and helium, provided a blow-down type wind tunnel. A solenoid-actuated eight inch pneumatic slide valve was used to control flow into the vacuum system.

### Gas Sample Collection System

The gas sample collection system consisted of a set of gas sampling bottles, a set of solenoid-operated three-way valves, a set of sampling probes, and the vacuum system just described.

The gas sampling bottles were made of glass with a stopcock at each end and had a volume of 70 ml. A set of probes were inserted in the flow field at various locations as shown in Figure 3. The probes were made of stainless steel tubing with an outside diameter of .032 inches (.022 inch inside diameter). The probes were centered between the walls of the test section and positioned parallel to the flow. The solenoid valves were connected between the probes and the sample bottles and were activated open

by the experimenter and closed simultaneously after sampling by a timed relay to obtain uniform sampling times. The vacuum system was used to evacuate the gas sample bottles simultaneously through a common manifold. A warning light indicated when the solenoid valves were open and a sample was being captured. A schematic of the gas sampling system is shown in Figure 6.

#### Pressure Measurements

The gas sampling probes were also used to measure the total pressure within the test section. The probes were connected to a set of vertical mercury manometers and employed the use of the solenoid valves to hold the pressure measurements until they could be manually recorded. Static pressure taps were located slightly upstream of each total pressure probe to avoid any interference of the detached shock wave from the probe tip. The initial pressure measurements were taken at a position 0.75 inches downstream of the nozzles and at one inch intervals thereafter as shown in Figure 3.

#### Instrumentation

The air stilling chamber pressure was measured with a 0-250 inch of Hg. dial gage accurate to within 0.4 inches of Hg. The helium stilling chamber pressure was measured with a similar dial gage (0-200 in Hg.) with the same accuracy.

Both stilling chamber temperatures were measured with copper/constantan thermocouples. The thermocouples were connected to a Honeywell strip-chart recorder using an ice bath as a reference. The accuracy of the temperature measuring system was  $\pm 2^{\circ}\text{F}$ .

Static pressures were measured on a vertical bank of U-tube mercury manometers. The measurements were recorded using a Graflex camera with a solenoid-activated shutter. The photographic results were read to an accuracy of 0.1 inch of Hg. with a 10 power viewing lens.

Total pressures were measured on a similar bank of U-tube mercury manometers. Because of the limits of the manometers, a provision was made to preload the reference side of the U-tube with a pressure above atmospheric (Fig 6). All measurements were read to the nearest 0.1 inch of Hg. By using the solenoid valves to take the total pressure measurements and capture the gas samples, the run time was reduced to a minimum, thus conserving the amount of helium used.

A 200 gram balance was used to weigh each gas sample container to an accuracy of .0001 grams. This weight was used to determine the mole fraction of each gas in the bottle. The pressure of each sample was taken using a low volume U-tube mercury manometer. The accuracy of these pressure measurements was 0.1 inch of Hg.

### III. Experimental Procedure

The experimental work was divided into three main areas; (1) visualization of the flow field using the schlieren system; (2) total and static pressure measurements at various stations downstream of the nozzles; and (3) gas sample collection and analysis.

Prior to each pressure measurement run, the air control valve and helium regulator were set to the desired pressures. The vacuum system was then evacuated to approximately 0.5 psia. Next, the pneumatic vacuum control valve was actuated open and the temperature recorder switched on. Airflow was initiated when the static pressures within the test section decreased indicating that the vacuum valve was open. Once the air stilling chamber pressure stabilized, the helium flow was initiated. Using the static pressures as an indication of stabilized flow, the solenoid valves were actuated to trap the total pressures when the vacuum system reached a pressure of 2 psia. The timer relay automatically closed the solenoid valve after 10 seconds and simultaneously activated the warning light. As the warning light illuminated, the camera's solenoid-operated shutter was tripped to photograph the static pressure manometer board. The helium flow, the air flow, and vacuum system were then stopped.

For the optical studies, the procedure used was exactly the same except that as the flow stabilized the room was darkened and the schlieren photograph taken approximately

eight seconds after actuating the solenoid valves. This prevented the warning light from interfering with the schlieren photograph. The exit plane static pressures were trapped by use of the solenoid valves.

Prior to each set of gas sample runs, the gas sample bottles were evacuated and weighed to determine the empty bottle weights. Once this had been done, the bottles were again evacuated to the same pressure and then isolated from the vacuum system by manually closing each stopcock that was connected to the vacuum. (A schematic of the gas sampling system is given in Figure 6). The gas collection procedure from this point was exactly the same as the procedure used to take the total pressure measurements. After the gas sample had been trapped, the stopcock on the other end of each bottle was closed manually and the bottles removed from the system for weighing. Each bottle was weighed within three minutes after capturing the sample and the weight recorded. The sample pressures were then measured by connecting a low volume manometer to one end of the bottle and opening the stopcock. The actual pressure that was in the bottle was calculated using the pressure read from the manometer. The mass and mole fraction of each gas was calculated using these weight and pressure measurements, the known temperature of the sample, and the known volume of each container. The method of making these calculations is given in Appendix A and B.

The total pressure of the helium and air was varied so as to give ten nozzle exit plane pressure ratios ( $P_r$ ) ranging from approximately 1.0 to 3.0. Pressure measurements and gas samples were taken at each position downstream of the nozzle exit for the ten pressure ratios. Ten schlieren photographs were made of the flowfield with the knife edge perpendicular to the flow direction and ten were made with the knife edge parallel to the flow direction. The ten photographs for each position of the knife edge correspond to the ten pressure ratios.

#### IV. Discussion of Results

The test equipment and instrumentation used in this study had previously been assembled by Carlile for use in a similar investigation. In order to become more familiar with its operation and the test procedures suggested by Carlile, the test equipment and instrumentation was evaluated before beginning this study. The evaluation checked instrumentation for accuracy, examined the sequencing of test procedures for best results, and checked some of the pressure measurements made by Carlile. The evaluation resulted in a few minor changes in equipment but overall accuracy of measurements and techniques presented by Carlile proved to be good.

##### Test Conditions

The Mach number at the exit plane of each nozzle was found using the exit plane static pressure and total pressure. The Mach numbers were found to be 2.9 for the air nozzle and 2.85 for the helium nozzle. Total pressures of the air and helium ranged from 45 to 110 psia and were varied to produce exit plane static pressure ratios from 1.0 to 3.0. Total temperature differences between the air and helium were small. Total temperatures varied between 74°F and 78°F and generally appeared to be the same as room temperature. Because of the relatively insignificant temperature differences, the exit velocity ratio was considered constant at 0.35.

### Pressure Measurement Analysis

The main purpose of the pressure measurement analysis was to determine if the flow field was symmetric about the center flow axis for different pressure ratios and different downstream positions. The results of these measurements are presented in graphical form in Figures 7, 8, 9, and 10. They show representative samples of the ratio of local total to local static pressures ( $P_t/P$ ) versus the non-dimensionalized y coordinate ( $y/D$ ). In addition, data stations in the y direction are numbered consecutively across the flow field from 1 to 9 (Fig 3). Lines that connect the data points were drawn to help visualize the symmetry. Figures 7 and 8 give  $P_t/P$  versus  $y/D$  for exit plane pressure ratios of 1.95 and 2.5 respectively for various positions downstream. Figures 9 and 10 give  $P_t/P$  versus  $y/D$  for  $x/D = 1.29$  and  $x/D = 4.74$  respectively at various pressure ratios. From this data it is apparent that the flow field is symmetric. This was important because symmetric boundary conditions for the center mixing layers was desired.

### Schlieren Analysis

The schlieren photographs of the flow field were enlarged 2.5 times the original size to provide ease in data reduction. The spreading angle ( $\theta$ ) of the helium to air mixing face was measured for all exit plane pressure ratios investigated and found to be constant at approximately three degrees (Fig 11). The spreading angle of the air to

helium mixing face could not be determined with any accuracy as the density gradients in the helium were not easily recognized in the schlieren photographs. Since the primary interest is in the mixing of the helium jet into the air jet, the analysis will use the center air jet in the flow field with helium jets bordering each side and thus will have two mixing regions as shown in Figure 11. It was found that as the exit plane pressure ratio was increased, the maximum width ( $w$ ) of the air jet core increased. Since the maximum core width is larger for higher values of  $Pr$ , the distance between mixing layers is greater. Therefore, the mixing of helium into the air jet doesn't take place as fast as it does at the lower values of  $Pr$ , even though the spreading angles are the same. Figures 12 through 15 are schlieren photographs of the flow field for various exit plane pressure ratios and knife edge configurations.

For a simplified analysis, assume that the spreading takes place linearly (Ref 11). The spreading angle can then be written as a function of distance downstream ( $x_m$ ) and the maximum core width ( $w$ ). Thus

$$\tan \theta = \frac{w/2}{(x_m - b)}$$

where  $x_m$  is the distance from the nozzle exit plane and  $b$  is the distance from the nozzle exit plane to the maximum core width (Figure 11). If  $\theta$  is constant, the distance downstream where the mixing layers meet will be a function of the

maximum core width and the distance  $b$ . The spreading angle has been shown to be a function of the velocity ratio of the two jets (Ref 9). In this study, the exit velocity ratio and  $\theta$  remained constant for all exit plane pressure ratios investigated. For mixing of the helium into the air jet to occur in a short distance downstream, the maximum width of the air jet core must be small. At this point it should be noted, if the air jet core is made smaller by reducing  $Pr$ , the helium core will become larger. Given this configuration, if the spreading angle of the air to helium face was the same as the spreading angle of the helium to air face for  $Pr = 1$ , the mixing layers for the helium nozzle would meet in a shorter distance than the mixing layers for the air nozzle (Fig 11). If  $Pr$  were less than 1.0, the air to helium mixing length would increase and the helium to air mixing length would decrease. Ideally, the best mixing would be when both mixing lengths were the same.

#### Gas Sampling Analysis

Gasdynamic lasers usually operate with a large number of alternating mixing nozzles. For a large array of nozzles, the mixing would be almost identical between any two nozzles. Since this investigation was limited to a small array of nozzles, the boundary layers on the upper and lower surfaces of the test section affect the mixing regions close to these surfaces. However, it was assumed that these boundary layer effects were negligible in the central

mixing regions. Thus, the central portion of the test section provided a good flow field for investigating the mixing characteristics. The mixing region between the center air nozzle and one of the bordering helium nozzles was analyzed. Gas mixture samples were collected across the mixing region at several positions downstream of the nozzles for exit plane pressure ratios ranging from 1.0 to 3.0. These samples were analyzed to determine the mole fraction of helium and air in each sample. The results of this analysis is given graphically in Figures 16 through 22.

Figure 16 is a plot of mole fraction of air ( $N_A$ ) and helium ( $N_H$ ) versus  $y/D$  for various exit plane pressure ratios. As  $Pr$  decreases for a fixed  $x/D$ , the mole fraction of helium in each sample increases, indicating greater mixing of the helium into the air jet, but less mixing of the air into the helium jet. This result is supported by the schlieren analysis.

Figures 17 through 22 are plots of mole fractions of air and helium versus exit plane pressure ratios at different positions downstream of the nozzles. The curve for  $y/D = -0.8$  (Sta # 3, centerline of helium nozzle) in Figure 17 shows the mole fraction of helium is relatively constant at a value of one and only decreases slightly for a decrease in  $Pr$ . As the distance downstream is increased (Fig 18-22), the curve for  $y/D = -0.8$  (Sta # 3) moves up, indicating a decrease in mole fraction of helium and thus better mixing. The curves for  $y/D = 0$  (Sta # 5, centerline of air nozzle)

changed very little as the distance downstream increased. However, as  $Pr$  decreased, the mole fraction of air decreased, indicating that for  $y/D = 0$  (Sta # 5), pressure ratio is more significant than downstream distance in the mixing process. The mole fraction of air at  $y/D = 0$  (Sta # 5) is never equal to one, even at  $x/D = 1.29$  (Pos A). This is due to the diffusion of helium into air. The curves for  $y/D = -0.4$  (Sta # 4) and  $y/D = 0.4$  (Sta # 6) behave like the curves for  $y/D = 0$  (Sta # 5) since the probes were aligned closer to the air jet than to the helium jet.

Distance downstream and exit plane pressure ratio are both factors in determining mixing of the helium and air jets. It is difficult to state which, if either, is the more important contributor to the mixing process, as complete mixing was not attained in the test section for any of the conditions investigated.

## V. Conclusions

This study was an investigation of two-dimensional supersonic jet mixing of helium and air using a given nozzle array. The following conclusions were reached as a result of this investigation:

1. Pressure measurements proved the flow field to be symmetric about the centerline of the center air nozzle.
2. The mixing was found to be a function of exit plane pressure ratio, the distance downstream, and relative nozzle size.
3. For exit plane pressure ratios ranging from 1.0 to 3.0, helium to air mixing increased for a decrease in exit plane pressure ratio. Air to helium mixing also increases for a decrease in exit plane pressure ratio, but not as rapidly.
4. Schlieren photographs of the flow field suggested that relative nozzle size would affect the mixing rate for a constant pressure ratio.
5. Mixing was found to increase with position downstream. Complete mixing was not possible in the test section used for this study at the pressure ratios investigated.

## VI. Recommendations

This study did not investigate the variation of velocity ratios or study exit plane pressure ratios below one. It is apparent that near  $Pr = 1.0$  there are greater changes in mole fractions for both gases. Also, since exit plane velocity ratios are reported to affect the spreading angle it most probably affects the mole fraction of the different gases. In order to learn more about these phenomena, the following studies are recommended:

1. An investigation of how velocity ratio affects mole fractions across the flow field at various downstream locations;
2. An investigation of exit plane pressure ratios below 1.0 and above 3.0;
3. Comparison of actual experimental work with an analytical model;
4. An investigation to determine how scaling the nozzles size up or down would affect mixing length;
5. An investigation of the mixing using higher Mach number nozzles.

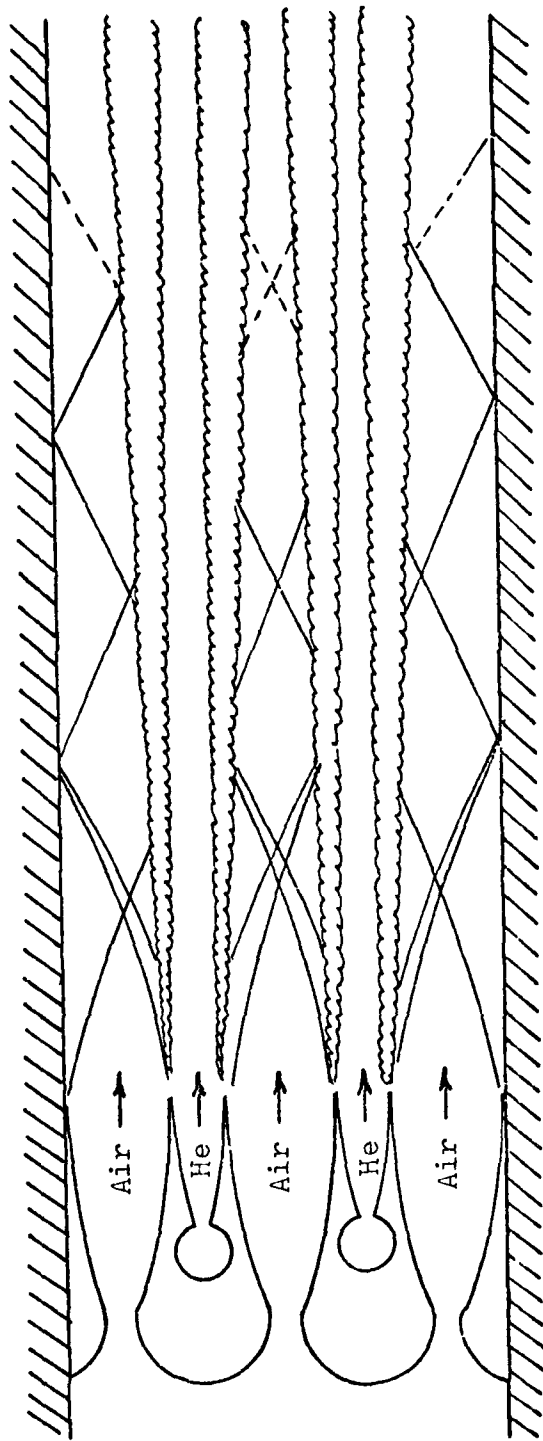
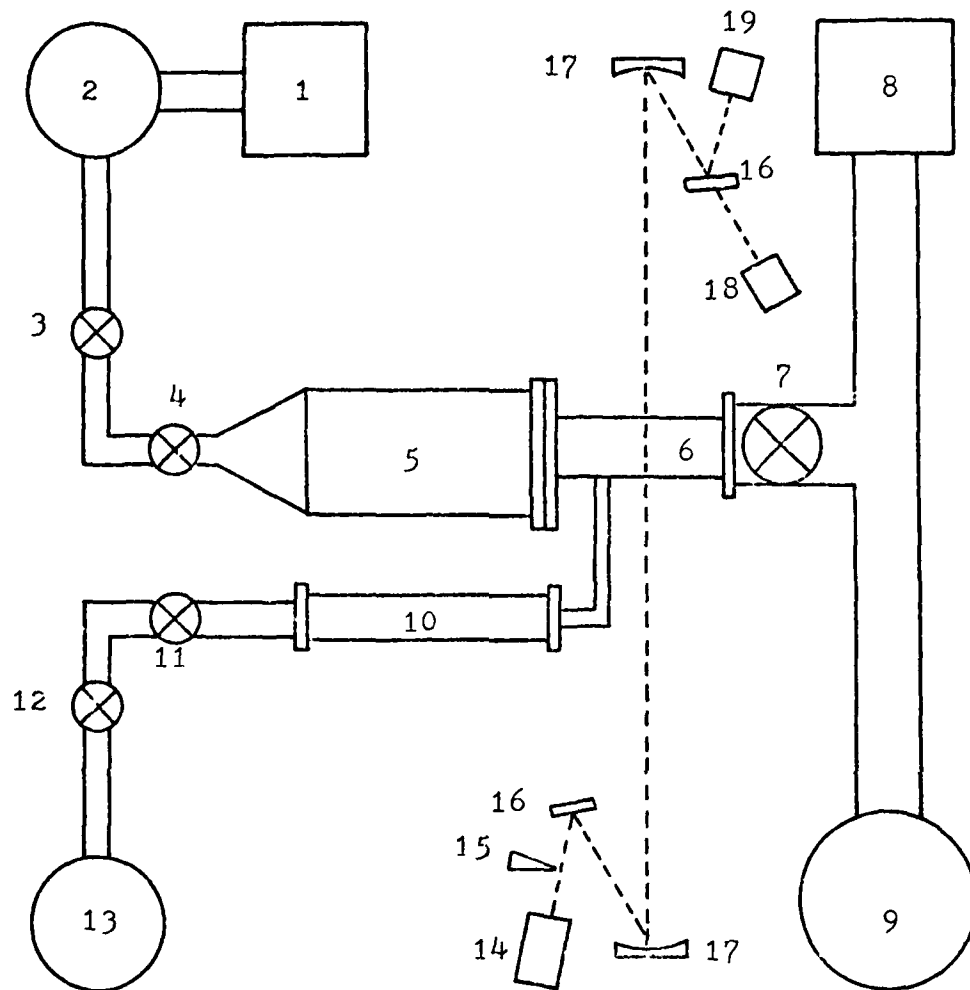


Fig. 1 Flow Field Schematic



- |                               |                           |
|-------------------------------|---------------------------|
| 1. Air Compressors and Dryers | 11. Hand Valve            |
| 2. Air Storage Tanks          | 12. Dome Regulators       |
| 3. Rotary Hand Valve          | 13. Helium Supply Bottles |
| 4. Slide Valve                | 14. Camera/View Screen    |
| 5. Air Stilling Chamber       | 15. Knife Edge            |
| 6. Test Section               | 16. Plane Mirror          |
| 7. Pneumatic Vacuum Valve     | 17. Parabolic Mirror      |
| 8. Vacuum Pumps               | 18. Steady Light Source   |
| 9. Vacuum Chambers            | 19. Spark Lamp            |
| 10. Helium Stilling Chamber   |                           |

Fig. 2 Test Equipment Schematic

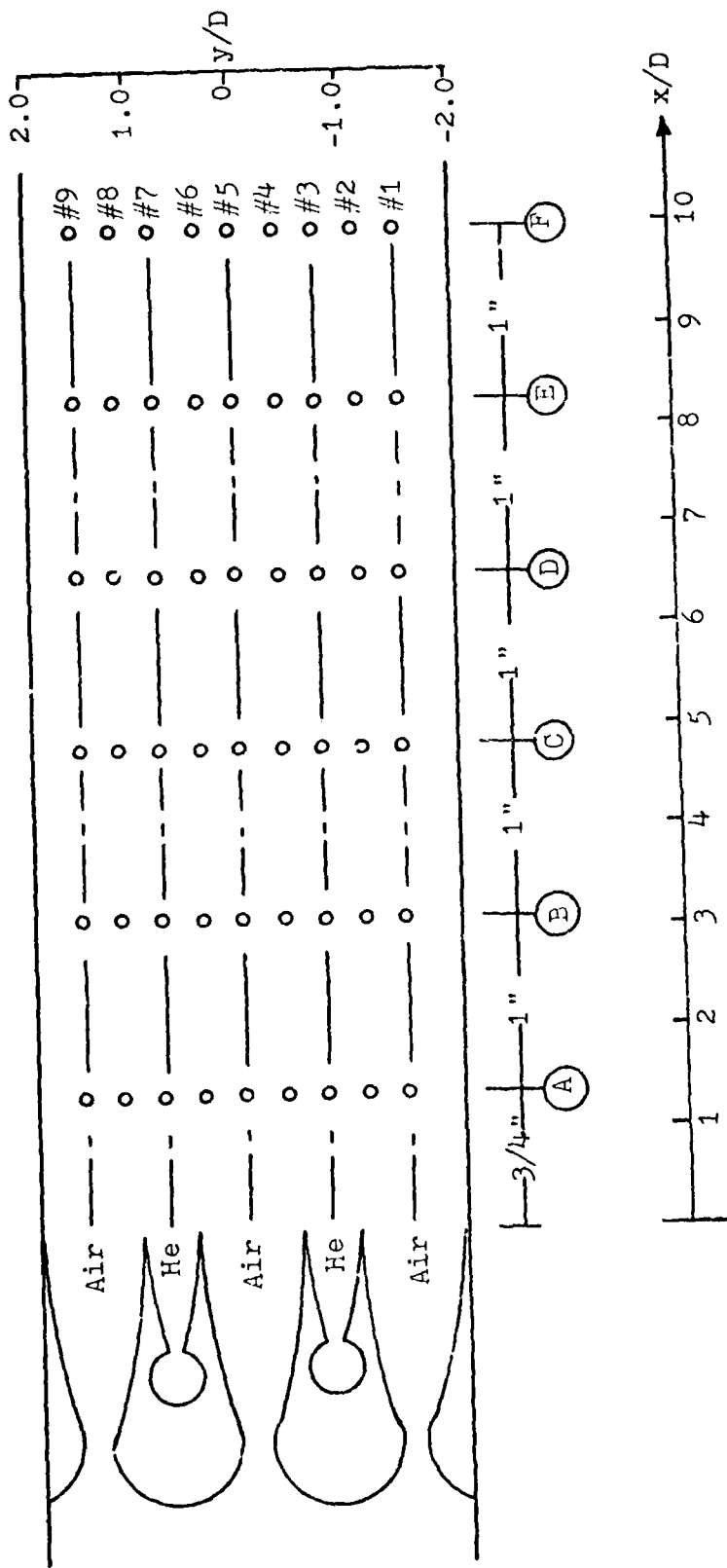


Fig. 3 Test Section Schematic Showing Probe Positions

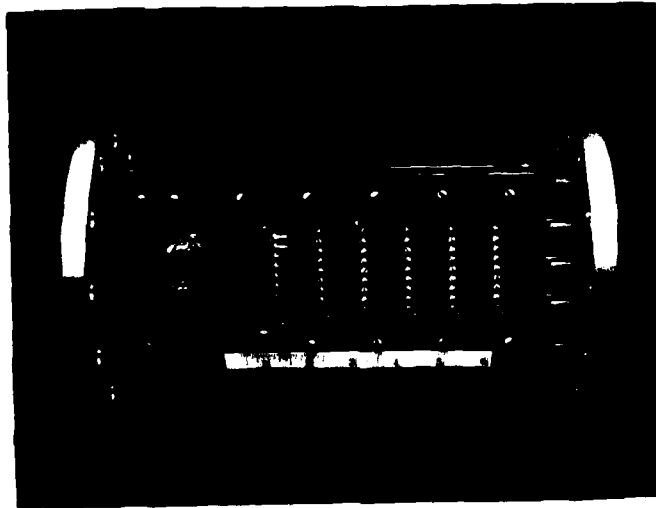


Fig. 4 Photograph of Test Section

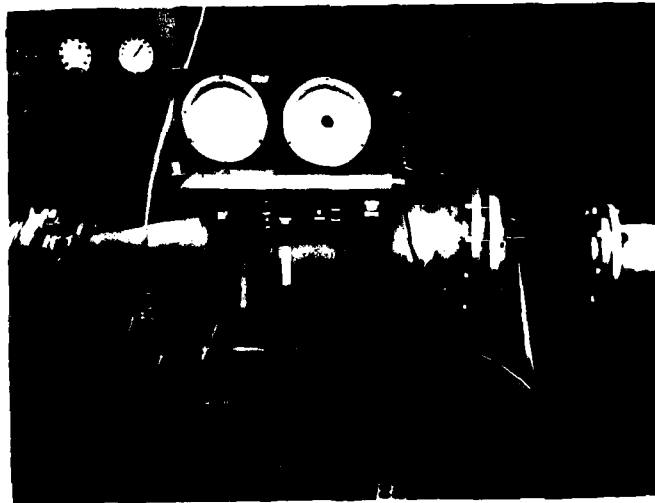


Fig. 5 Photograph of Test Apparatus

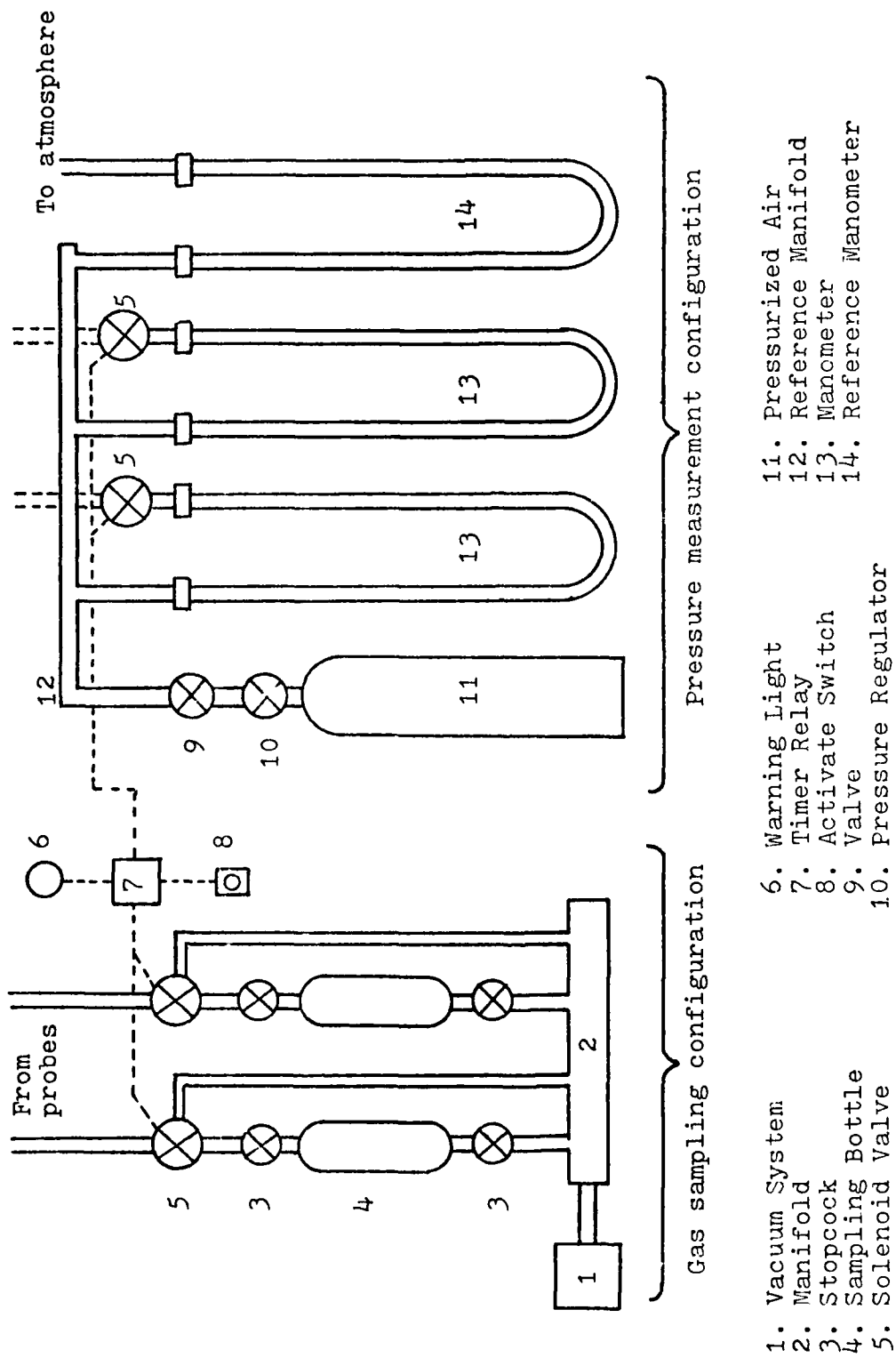


Fig. 6 Gas Sampling and Pressure Measurement Configuration

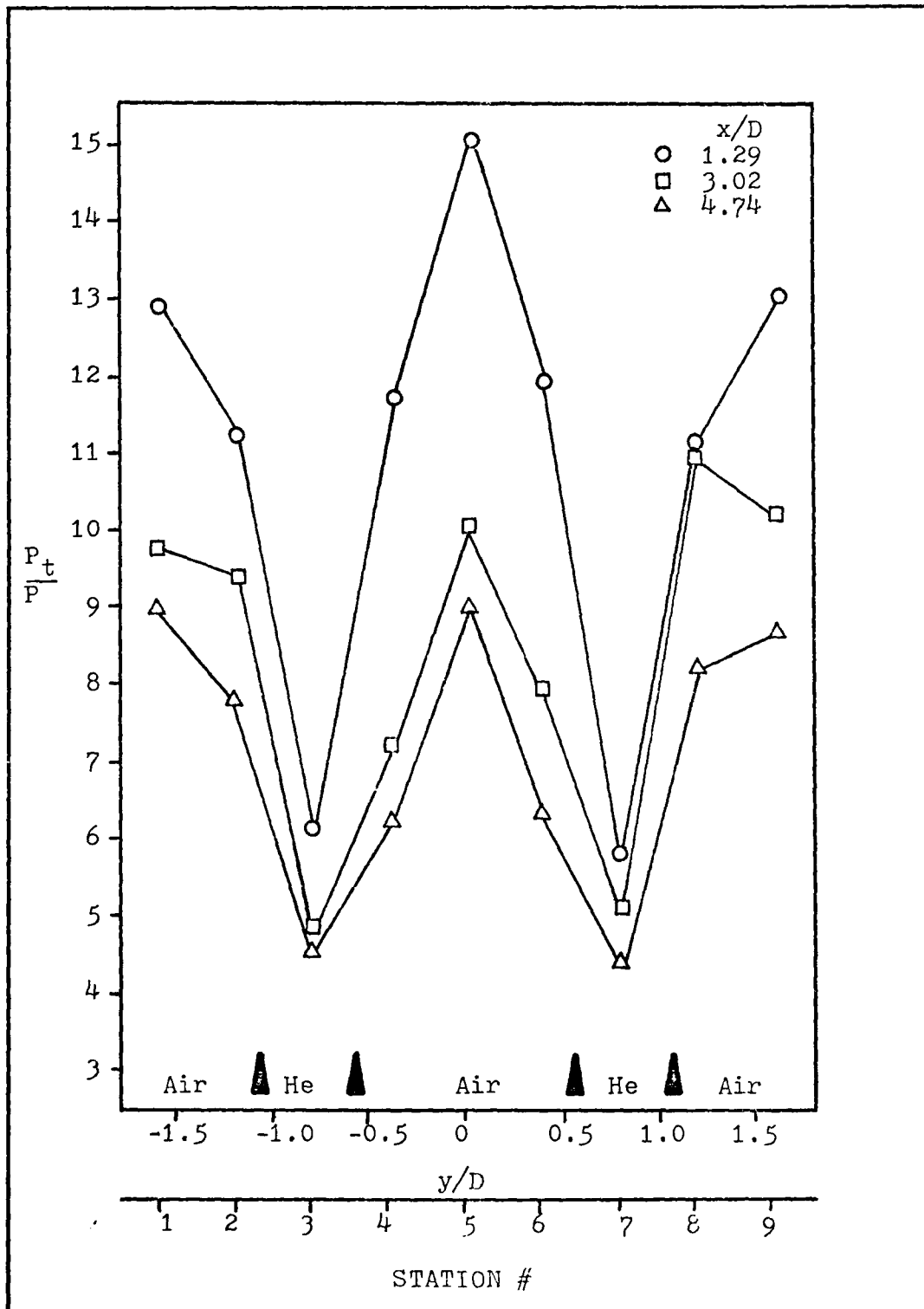


Fig. 7 Variation of  $P_t/P$  Across the Flow Field for Several Downstream Locations,  $Pr = 1.95$

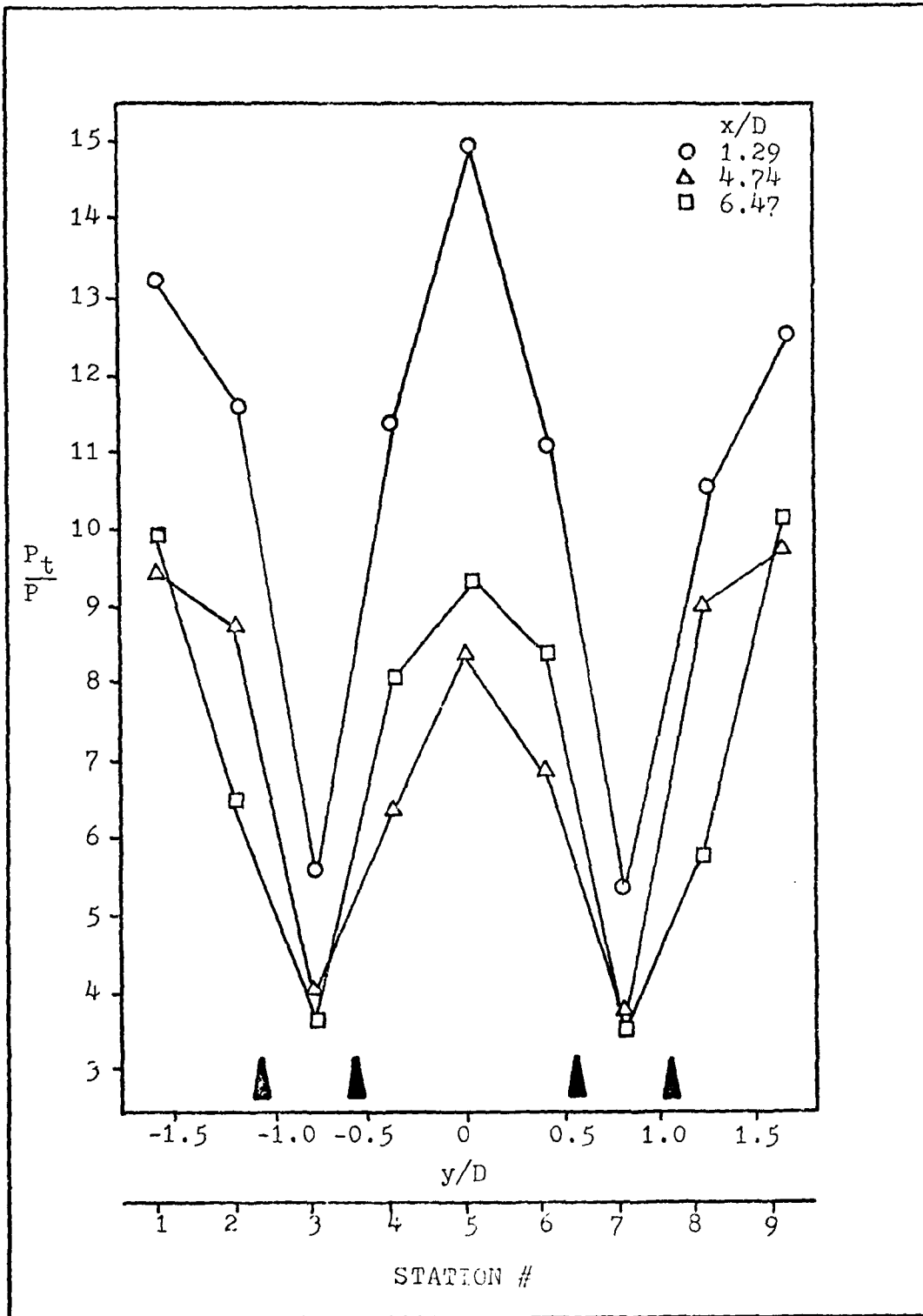


Fig. 8 Variation of  $P_t/P$  Across the Flow Field for Several Downstream Locations,  $Pr = 2.50$

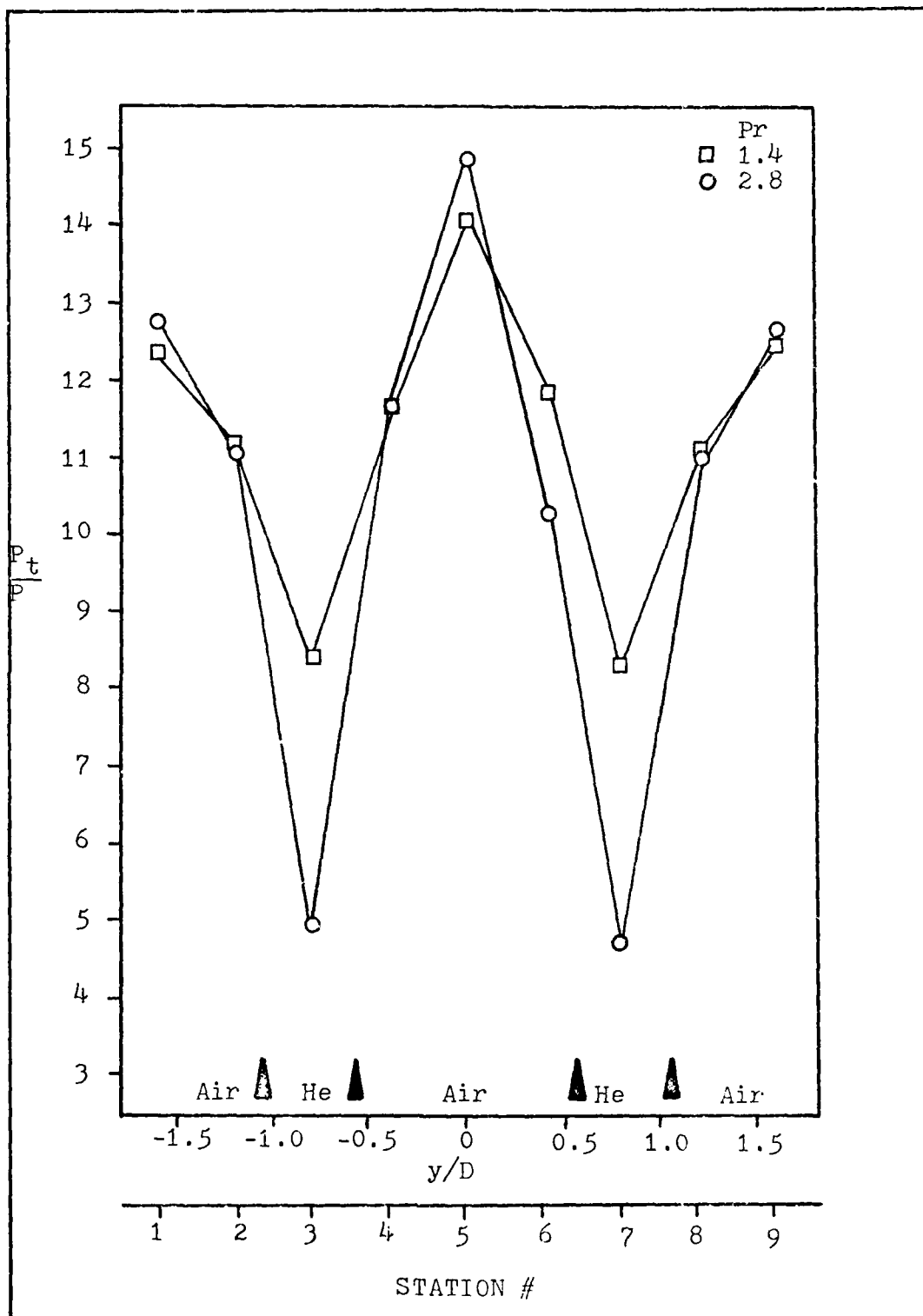


Fig. 9 Variation of  $P_t/P$  Across the Flow Field for Several Exit Plane Pressure Ratios,  $x/D = 1.29$  (Position A)

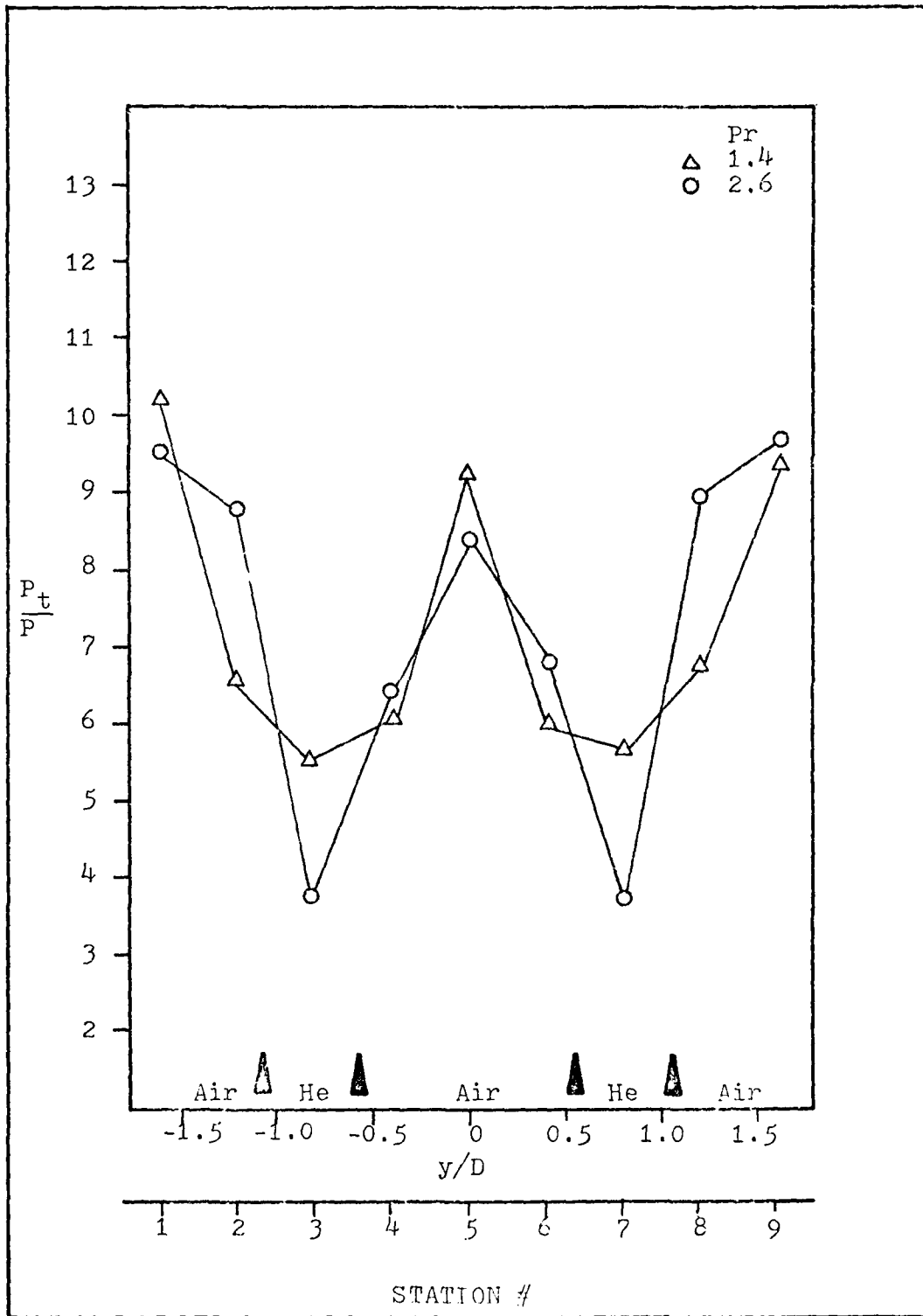


Fig. 10 Variation of  $P_t/P$  Across the Flow Field for Several Exit Plane Pressure Ratios,  $x/D = 4.74$  (Position C)

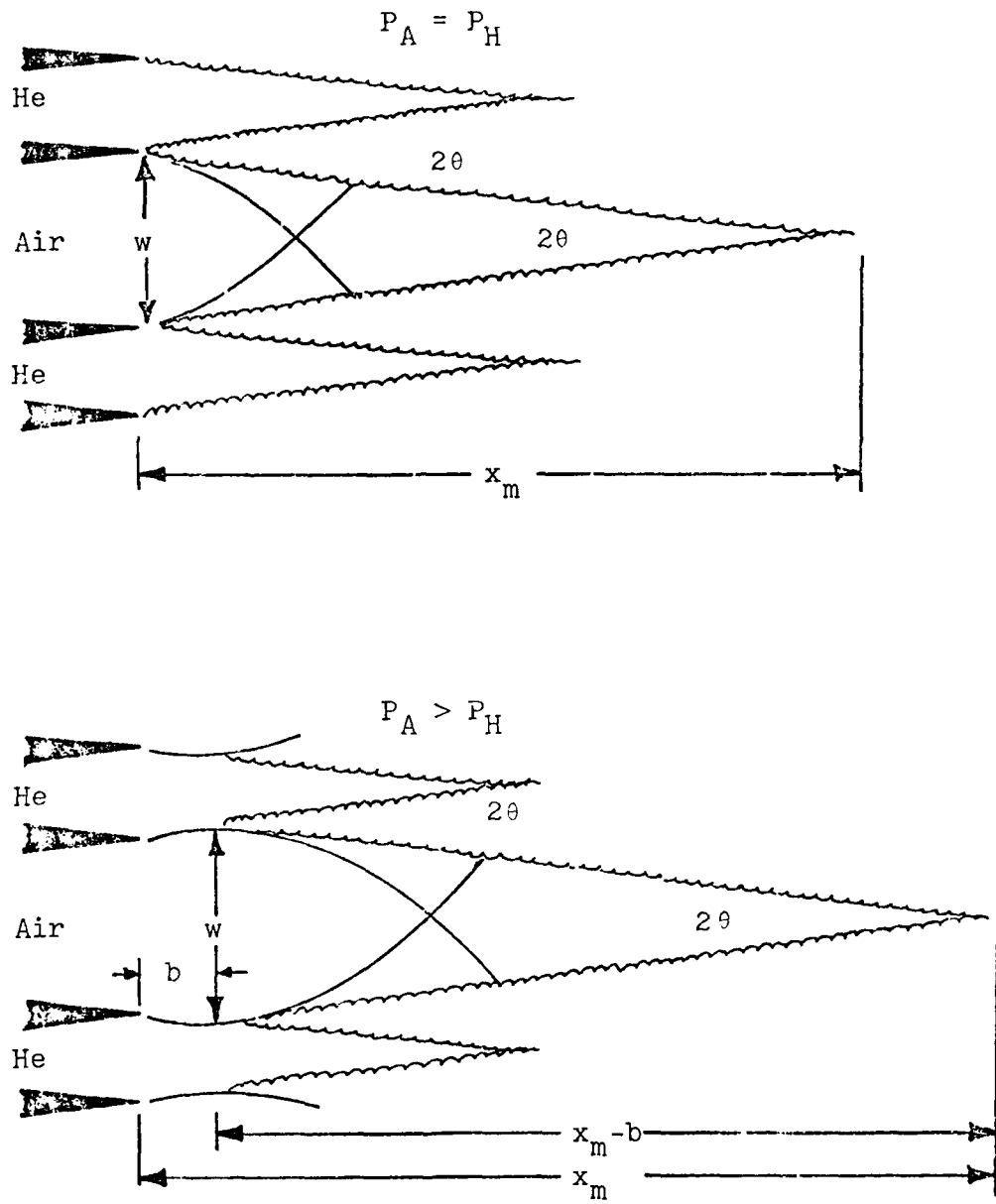


Fig. 11 Mixing Geometry and Jet Core Schematic.

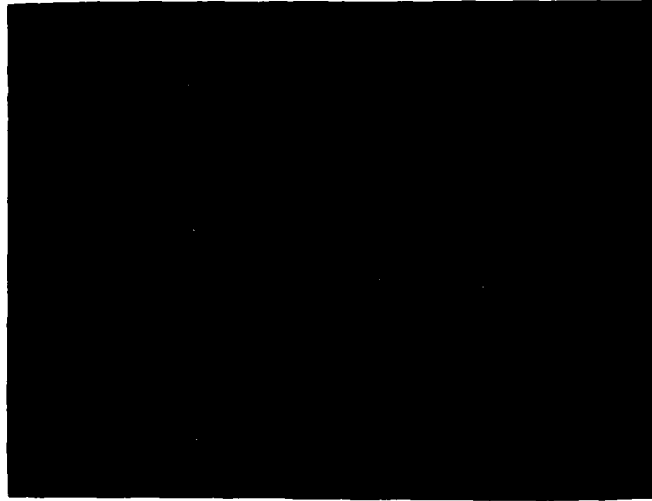


Fig. 12 Schlieren Photograph of Flow Field,  $Pr = 2.0$ ,  
Knife Edge Perpendicular to Flow.

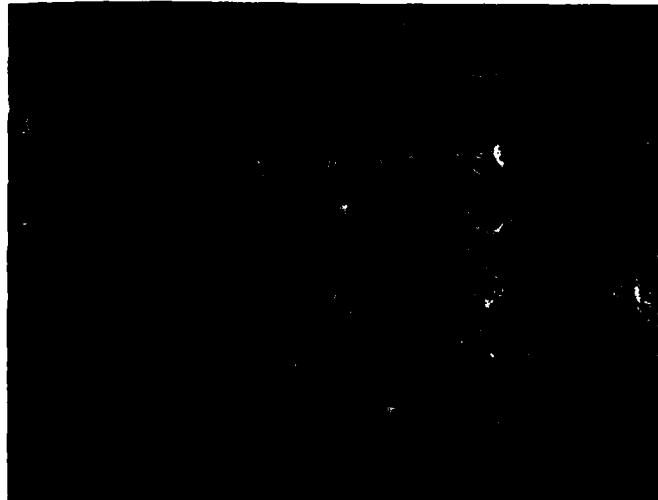


Fig. 13 Schlieren Photograph of Flow Field,  $Pr = 2.5$ ,  
Knife Edge Perpendicular to Flow.

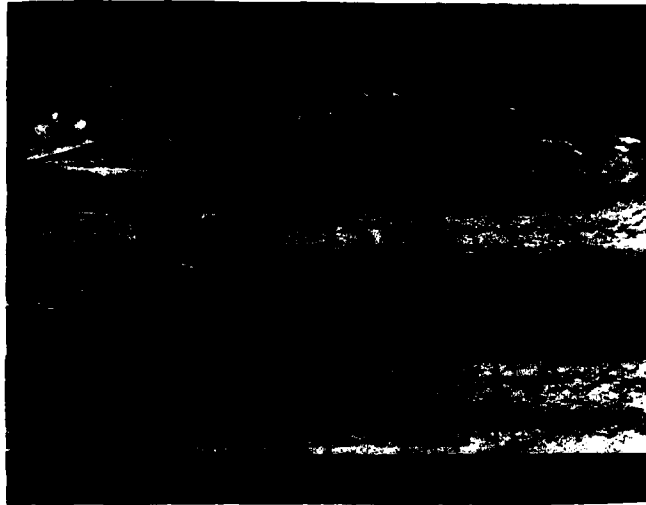


Fig. 14 Schlieren Photograph of Flow Field,  $Pr = 1.3$ ,  
Knife Edge Parallel to Flow.



Fig. 15 Schlieren Photograph of Flow Field,  $Pr = 2.8$ ,  
Knife Edge Parallel to Flow.

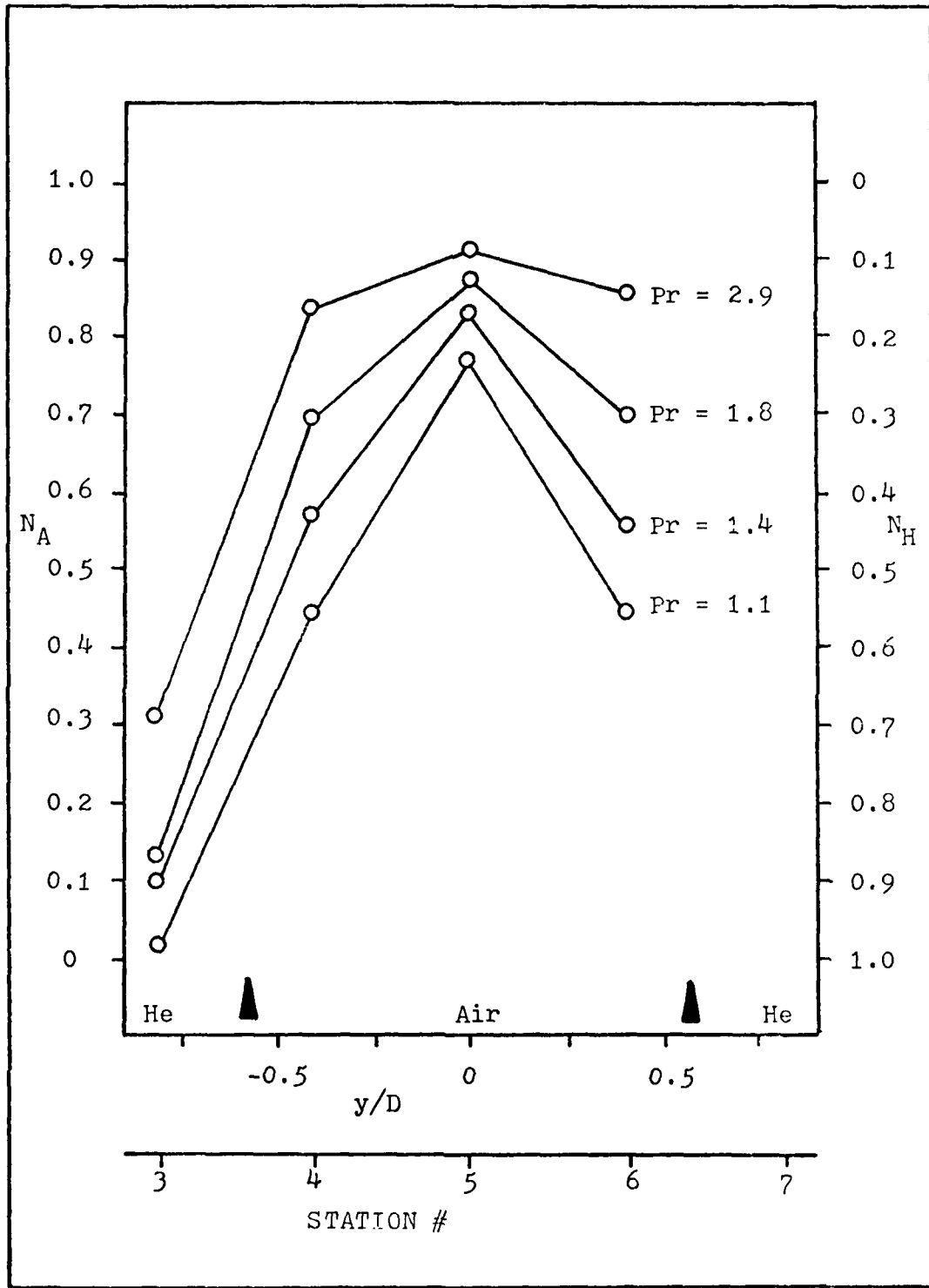


Fig. 16 Mole Fraction Variation of Air and Helium Across Flow Field for Several Values of Exit Plane Pressure Ratios,  $x/D = 6.47$  (Position D).

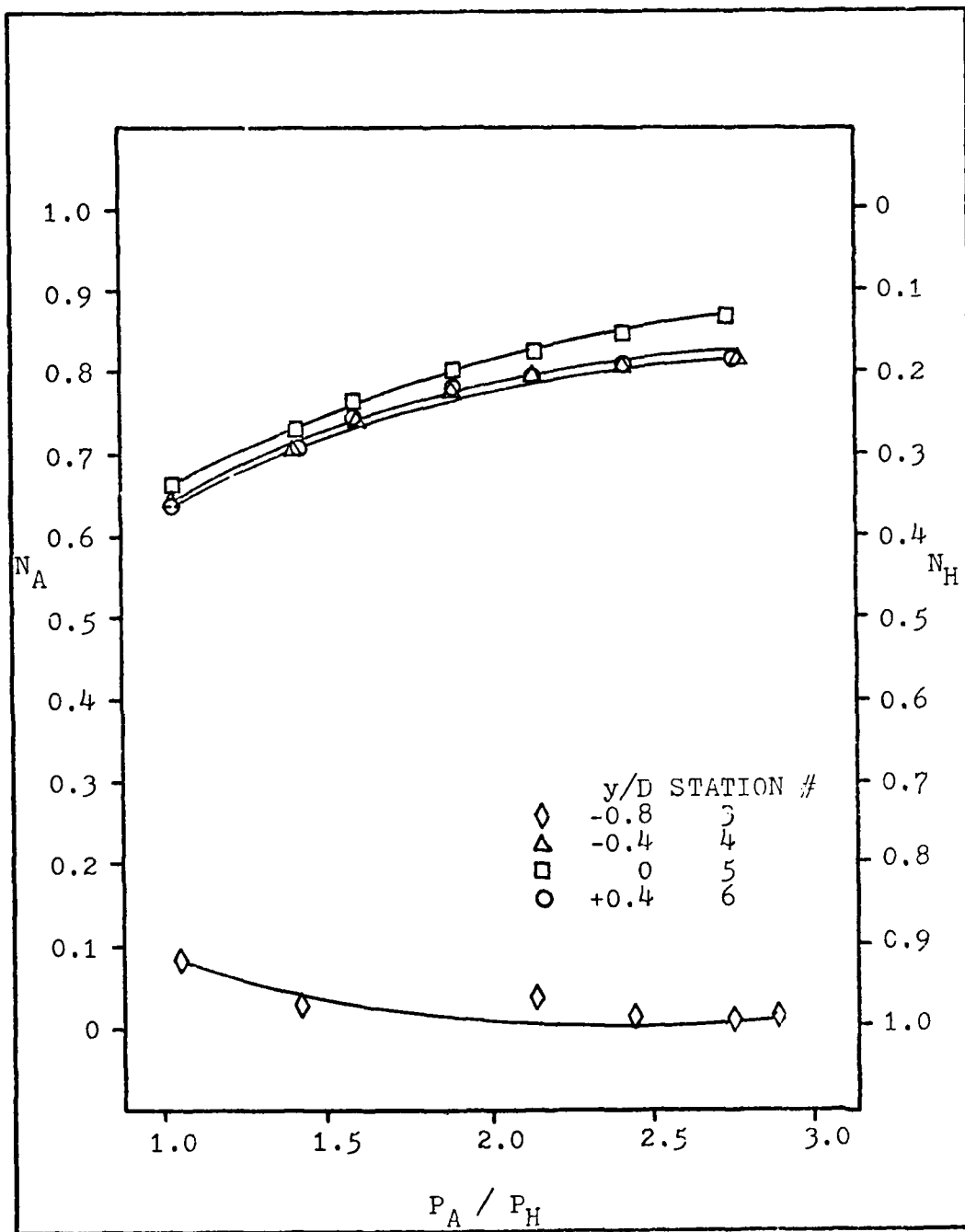


Fig. 17 Mole Fraction Variation of Air and Helium with Exit Plane Pressure Ratios,  $x/D = 1.29$  (Position A)

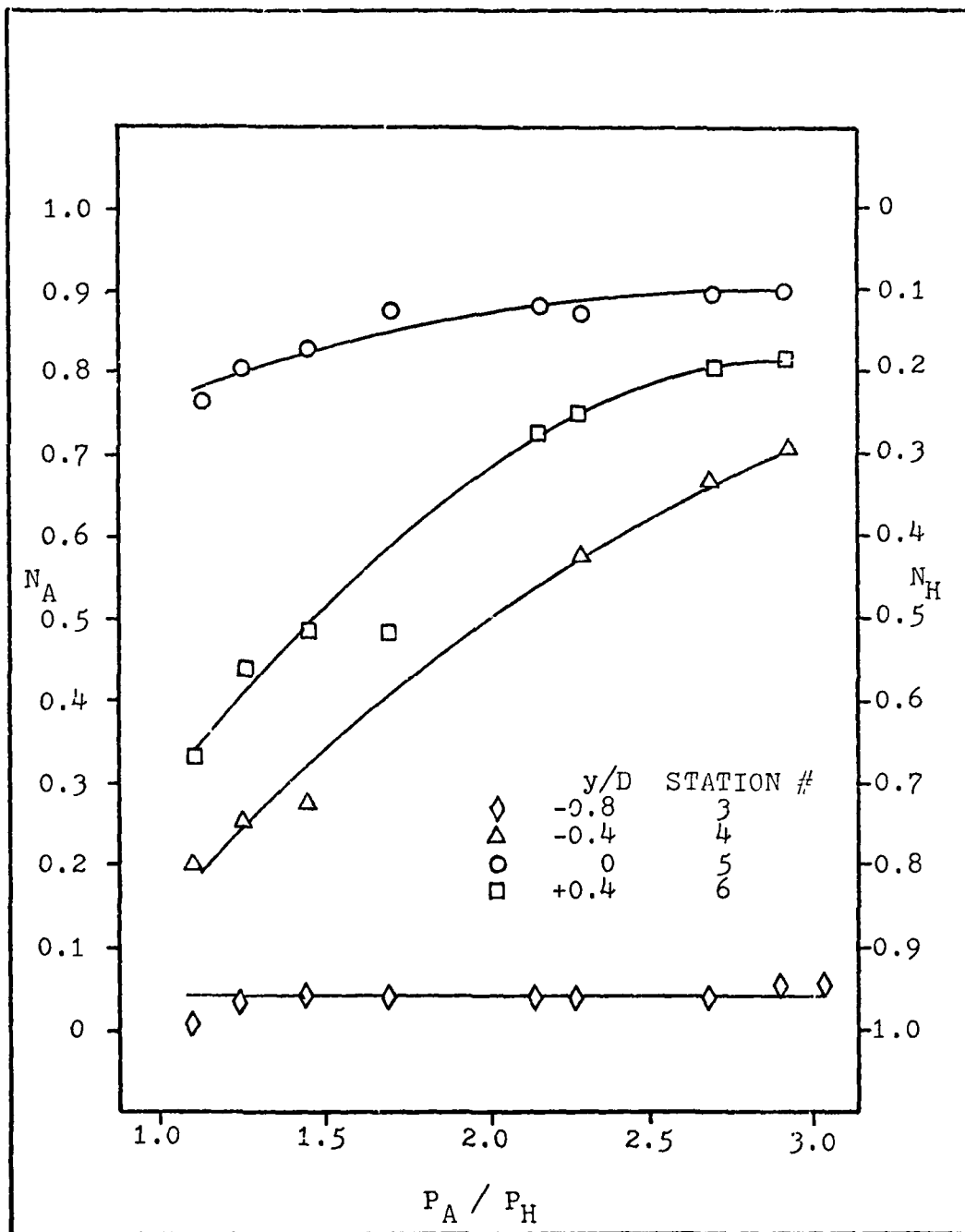


Fig. 18 Mole Fraction Variation of Air and Helium with Exit Plane Pressure Ratios,  $x/D = 3.02$  (Position B)

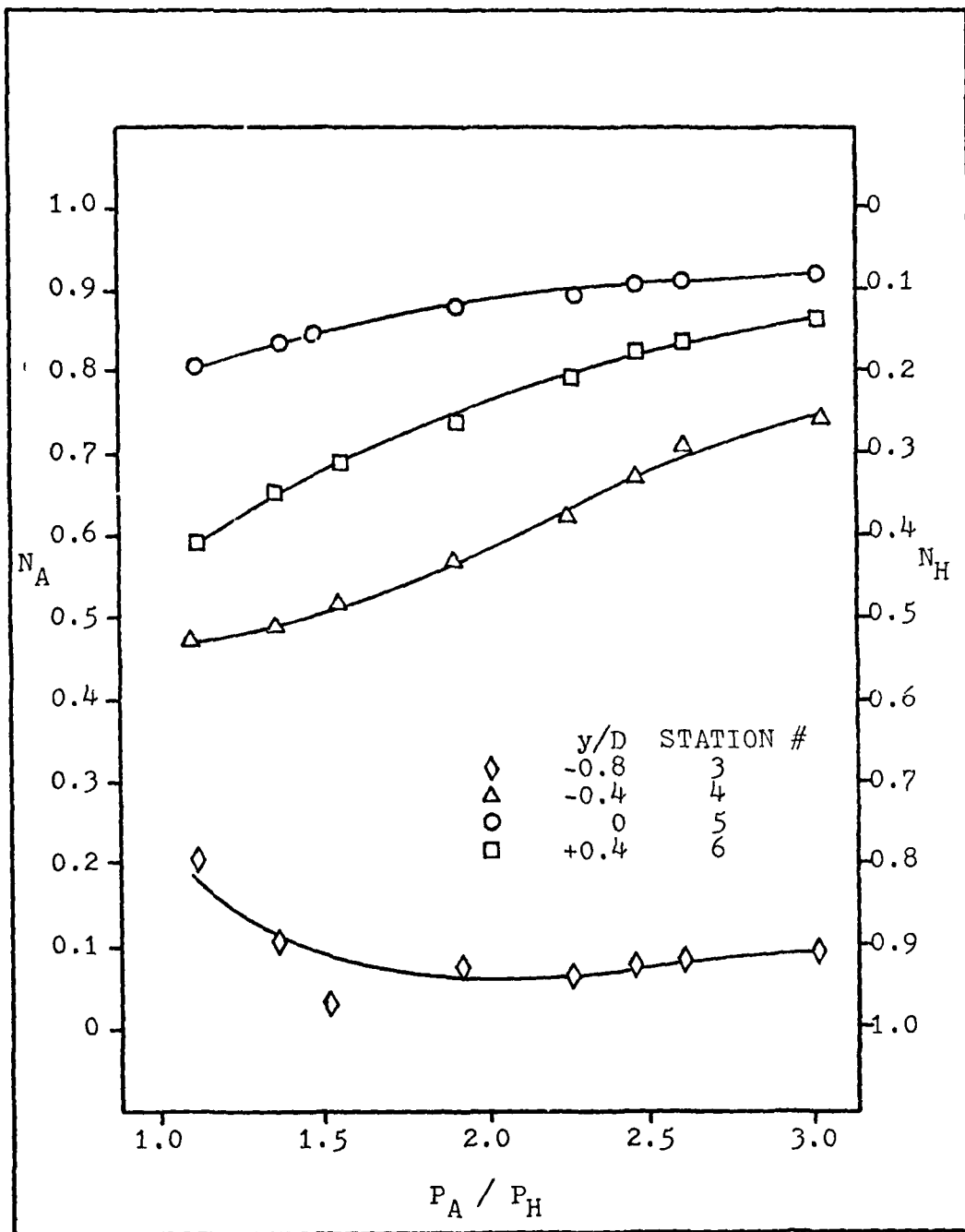


Fig. 19 Mole Fraction Variation of Air and Helium with Exit Plane Pressure Ratios,  $x/D = 4.74$  (Position C)

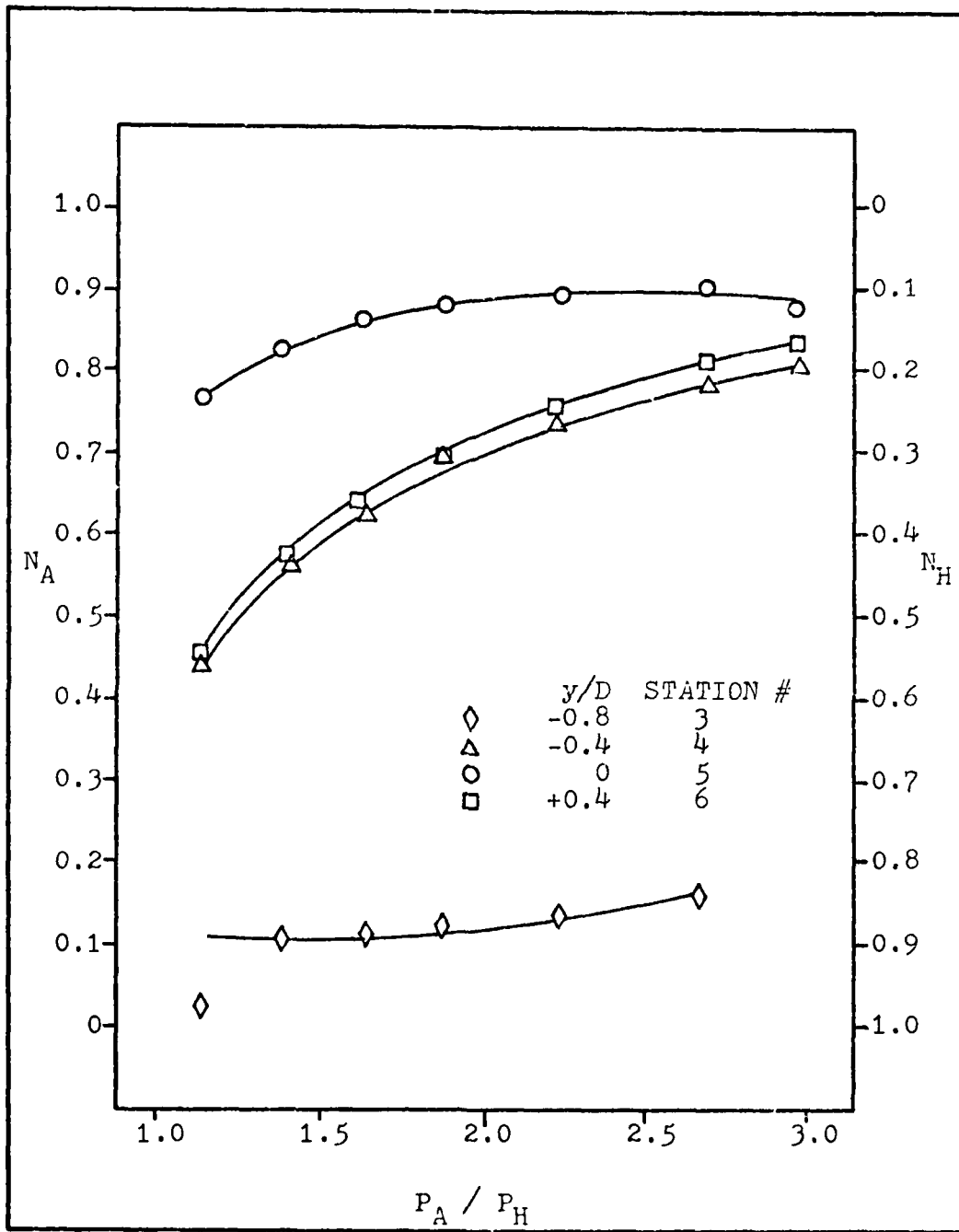


Fig. 20 Mole Fraction Variation of Air and Helium with Exit Plane Pressure Ratios,  $x/D = 6.47$  (Position D)

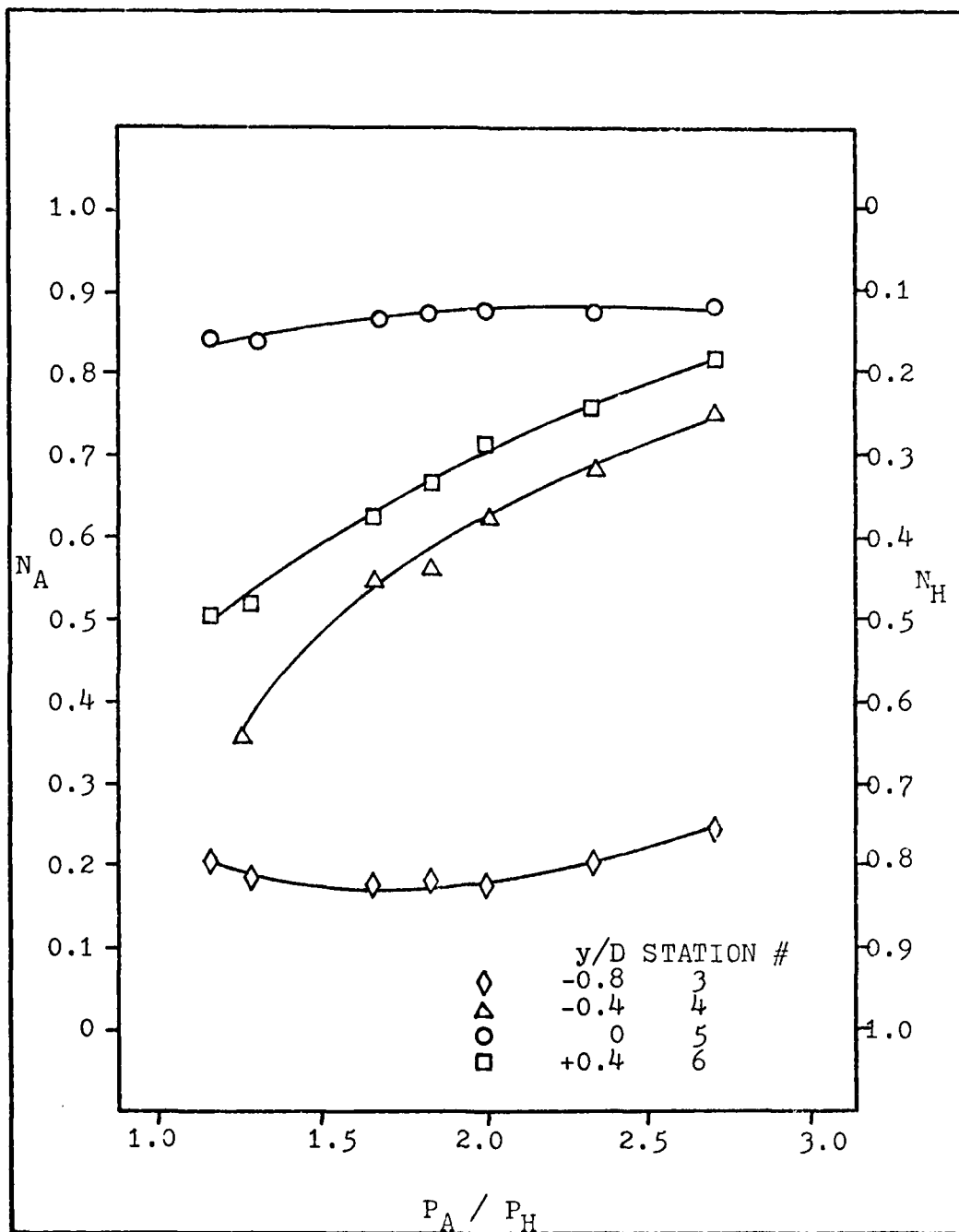


Fig. 21 Mole Fraction Variation of Air and Helium with Exit Plane Pressure Ratios,  $x/D = 8.19$  (Position E)

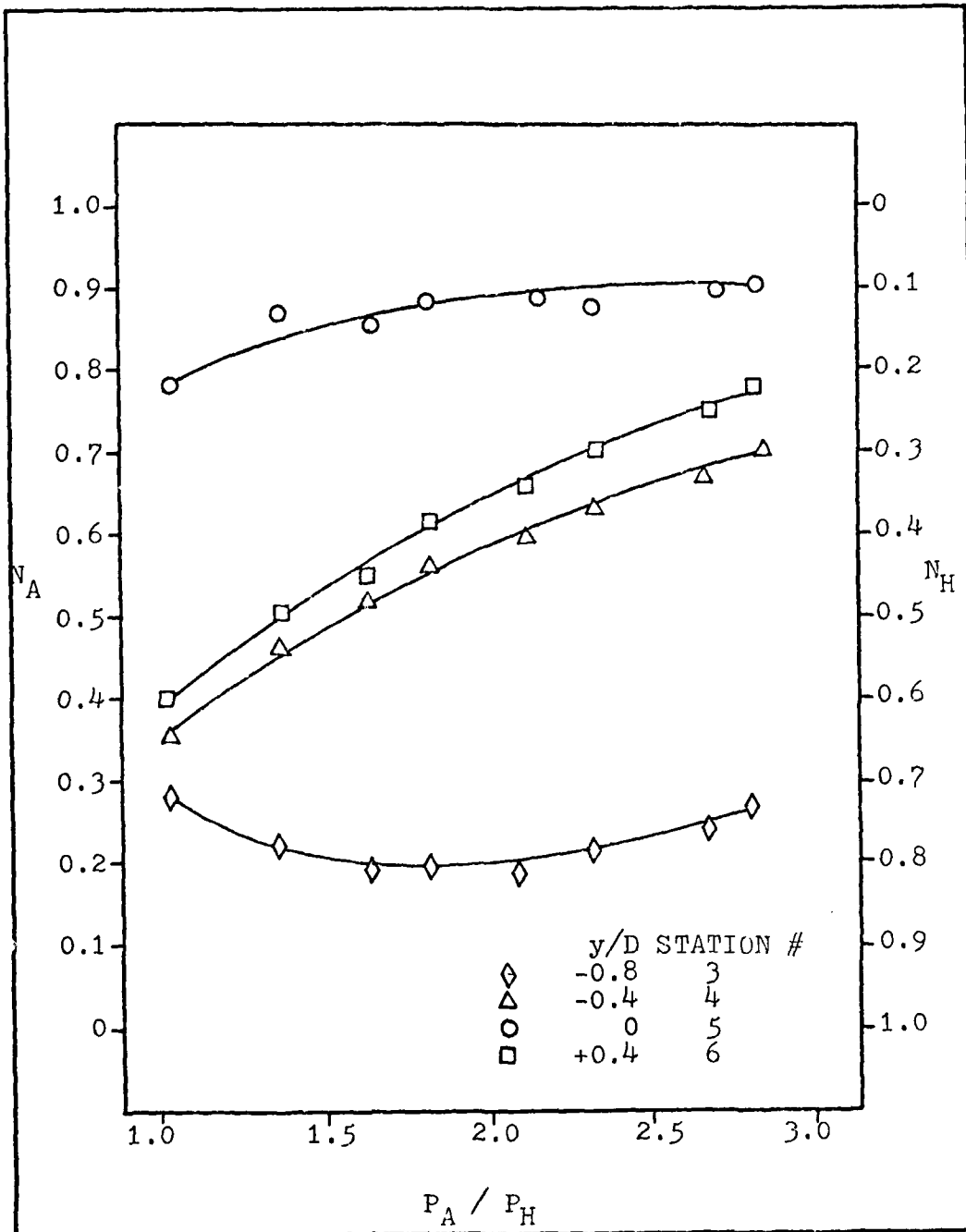


Fig. 22 Mole Fraction Variation of Air and Helium with Exit Plane Pressure Ratios,  $x/D = 9.91$  (Position F)

## References

1. Gerry, Edward T. "Gasdynamic Lasers," IEEE Spectrum, Volume 7, pp. 51-58, Nov 1970.
2. Anderson, John D. Gasdynamic Lasers: An Introduction New York: Academic Press, 1976.
3. O'Shea, D. C., et al. Introduction to Lasers and Their Applications. Menlo Park, California: Addison
4. Borgi, R., et al. "Supersonic Mixing Nozzle for Gasdynamic Lasers." Applied Phys Letts, Volume 22, No. 12, June 1973.
5. Cassidy, P., et al. "A New Mixing Gasdynamic Laser," AIAA Journal, Volume 16, No. 4, pp. 305-312, April 1978.
6. Peterson, C. W. "Measurements of Flow-Field Properties in a Gasdynamic Laser Nozzle Wake," Proceedings of AIAA 11th Fluid and Plasma Dynamics Conference. AIAA Report 78-1214. New York: American Institute of Aeronautics and Astronautics.
7. Bauer, R. C., "An Analysis of Two-Dimensional Laminar and Turbulent Compressible Mixing," AIAA Journal, Volume 4, No. 3, March 1966.
8. Donaldson, Coleman. "Theoretical and Experimental Investigation of the Compressible Free Mixing of Two Dissimilar Gases," AIAA Journal, Volume 4, No. 11, November 1966.
9. Forde, J. M. "The Mixing of Turbulent Supersonic Fuel-Air Streams," The Aeronautical Quarterly, Volume 1, pp. 377-387, Nov 1965.
10. Carlile, John D. Design and Evaluation of a Facility to Study Two-Dimensional Supersonic Air-Helium Mixing. MS Thesis. Wright-Patterson AFB, Ohio: Air Force Institute of Technology, December 1975.
11. Schlichting, Hermann. Boundary Layer Theory (Sixth Edition). New York: McGraw-Hill Book Company, 1968.
12. Timm, John A. General Chemistry. New York: McGraw-Hill Book Company, 1966.
13. Liepman, H. W., and A. Roshko. Elements of Gasdynamics. New York: John Wiley and Sons, Inc., 1957.

## Appendix A

### Gas Sample Pressure Calculation

A low volume U-tube mercury manometer was used to measure the pressure in the gas sample bottles. However, the pressure read from the manometer was not the actual pressure in the bottle. In order to eliminate this error, the actual pressure was calculated using the following method. The bottle was connected to the manometer as shown in Figure A1 and the stop cock opened. Since the space between the mercury surface and gas sample bottle was at atmospheric pressure, it either added or subtracted from the pressure actually in the bottle. To compensate for this, the total mixture in the bottle was assumed to be the same as the total mixture in the bottle and manometer tube when the bottle was opened. This was reasonable since the volume of the manometer tube was small as compared to the volume of the bottle. Thus

$$p_1 V_1 = \text{constant} = p_2 V_2 \quad (\text{A.1})$$

where

$p_1$  = pressure of bottle and manometer combined

$p_2$  = pressure of bottle alone

$V_1$  = volume of bottle and manometer combined

$V_2$  = volume of bottle alone

The volume  $V_2$  of each bottle was determined by filling it with water and weighing it. Using the density of water to be one gram per cubic centimeter, the volumes were calculated (Ref 12). The volume  $V_1$  was calculated from the following relation:

$$V_1 = V_2 + A (h_0 + \frac{h}{2}) \quad (A.2)$$

where

A = volume per inch of manometer

h = pressure in inches of mercury

$h_0$  = distance in inches from bottle to zero position of manometer (Fig A1).

From the equations above, the pressure was given by

$$P_2 = \frac{P_1 V_1}{V_2} = \frac{P_1 [ V_2 + A (h_0 + \frac{h}{2}) ]}{V_2} \quad (A.3)$$

Known pressures that were placed in the bottles were compared with pressures calculated using equation A.3. The calculated pressures were found to have an accuracy of approximately  $\pm 2\%$  of the known pressure.

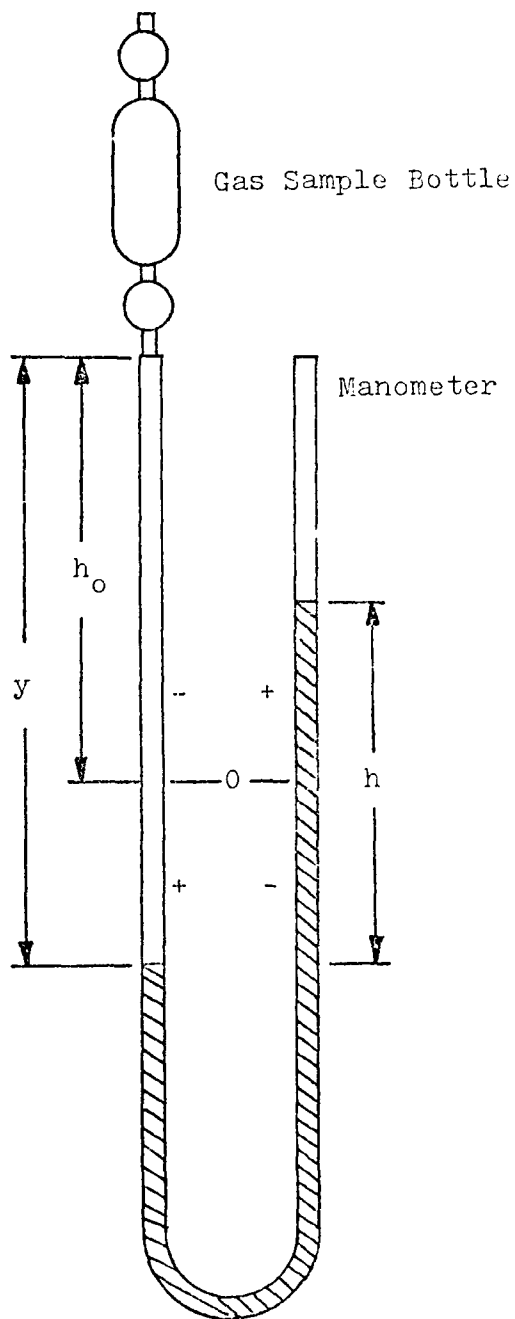


Fig. A1 Schematic of Gas Sample Bottle Pressure Measurement Configuration

## Appendix B

### Calculation of Masses and Mole Fractions

The mass of the gas mixture was found by subtracting the empty bottle weight from the sample bottle weight. From the pressure, volume, and temperature measurements, the mass of 100% helium and 100% air was calculated using the equation of state for an ideal gas (Ref 13).

Next, the following set of equations were solved for percent of helium and air:

$$M_A m_A + M_H m_H = m_T \quad (\text{B.1})$$

$$M_A + M_H = 1.0 \quad (\text{B.2})$$

where

$M_A$  = percent of air by mass

$m_A$  = mass of 100% air

$M_H$  = percent of helium by mass

$m_H$  = mass of 100% helium

$m_T$  = mass of gas mixture

Once the percents of helium and air were calculated, the actual mass of each was found by simply multiplying the percentage value times the 100% value. The number of moles of each gas was determined by dividing its mass by molecular weight from which the mole fraction of each gas was calculated (Ref 12).

### Vita

Roy L. Bonney, Jr., was born on 11 February 1949 in Norfolk, Virginia, the son of Roy L. and Gladys B. Bonney. He graduated from high school in South Hill, Virginia in 1966 and attended Virginia Polytechnic Institute where he received his Bachelor of Science degree in Aerospace Engineering in June 1970. He was a Civil Engineer for the City of Chesapeake for several months prior to entering active duty in the Air Force. He was married to Carol Esther Townsend in September 1970 at Portsmouth, Virginia. In November 1970 he entered active duty at Laughlin AFB, Texas, for Undergraduate Pilot Training. Upon completion of pilot training he remained at Laughlin as a T-37 instructor pilot until May of 1975. He was transferred to Pope AFB, North Carolina and served with the 39th Tactical Airlift Squadron as a C-130E Aircraft Commander. He remained at Pope AFB until entering the Air Force Institute of Technology in June of 1977. Upon completion of the AFIT program he will be assigned to the Flight Dynamics Lab at Wright-Patterson AFB, Ohio.

Permanent Address: 107 Shore Drive

Portsmouth, Virginia 23701

UNCLASSIFIED

SECURITY CLASSIFICATION OF THIS PAGE (When Data Entered)

REPORT DOCUMENTATION PAGE		READ INSTRUCTIONS BEFORE COMPLETING FORM
1. REPORT NUMBER AFIT/GAM/AA/78D-2	2. GOVT ACCESSION NO.	3. REPORT'S CATALOG NUMBER
4. TITLE (and Subtitle) TWO-DIMENSIONAL SUPERSONIC JET MIXING OF AIR AND HELIUM		5. TYPE OF REPORT & PERIOD COVERED MS Thesis
7. AUTHOR(s) Roy L. Bonney Captain USAF		6. PERFORMING ORG. REPORT NUMBER
9. PERFORMING ORGANIZATION NAME AND ADDRESS Air Force Institute of Technology (AFIT-EN) Wright-Patterson AFB, Ohio 45433		8. CONTRACT OR GRANT NUMBER(S)
11. CONTROLLING OFFICE NAME AND ADDRESS		10. PROGRAM ELEMENT, PROJECT, TASK AREA & WORK UNIT NUMBERS
		12. REPORT DATE December 1978
		13. NUMBER OF PAGES 57
14. MONITORING AGENCY NAME & ADDRESS (if different from Controlling Office)		15. SECURITY CLASS. (of this report) Unclassified
		15a. DECLASSIFICATION/DOWNGRADING SCHEDULE
16. DISTRIBUTION STATEMENT (of this Report)  Approved for public release; distribution unlimited		
17. DISTRIBUTION STATEMENT (of the abstract entered in Block 20, if different from Report)		
18. SUPPLEMENTARY NOTES Approved for public release; IAW AFR 190-17  JOSEPH P. HIPPS, Major, USAF Director of Information		
19. KEY WORDS (Continue on reverse side if necessary and identify by block number) Supersonic Mixing Mixing in a Gasdynamic Laser Parallel Stream Mixing Mixing of Helium and Air		
20. ABSTRACT (Continue on reverse side if necessary and identify by block number) This study investigated the mixing and flow field characteristics of helium and air using an array of two-dimensional Mach 3.0 nozzles. The study made use of schlieren photography, pressure measurements, and gas sampling for the analysis. Exit plane pressure ratios from 1.0 to 3.0 were investigated. Exit velocity ratios were assumed constant for all test conditions. Test equipment consisted of the nozzle array installed in a blow-down type system. Static pressure taps and total pressure		

DD FORM 1473  
1 JAN 73

EDITION OF 1 NOV 65 IS OBSOLETE

UNCLASSIFIED

SECURITY CLASSIFICATION OF THIS PAGE (When Data Entered)

UNCLASSIFIED

SECURITY CLASSIFICATION OF THIS PAGE (When Data Entered)

probes were installed in the flow field downstream of the mixing nozzles to measure pressures. The probes were also used to capture gas samples. Pressure measurement results showed symmetry of the flow field. Gas samples and schlieren analysis indicated that mixing was a function of exit plane pressure ratio and distance from nozzle exit.

UNCLASSIFIED

SECURITY CLASSIFICATION OF THIS PAGE (When Data Entered)